Effects of oxy-enriched oxidizer and nitrous oxide addition on characteristics of laminar methane jet diffusion flame

Hsien-Tsung Lin[1], Guan-Bang Chen[2], Tsarng-Sheng Cheng[3], Yueh-Heng Li[1], Yei-Chin Chao[1]
[1]Department of Aeronautics and Astronautics, National Cheng Kung University,
Tainan, 701, Taiwan
[2]Research Center of Energy Technology and Strategy, National Cheng Kung University,
Tainan, 701, Taiwan
[3]Department of Mechanical Engineering, Chung Hua University,
Hsinchu, 300, Taiwan

Keywords: Methane diffusion flame, oxy-combustion, inverse diffusion flames, nitrous oxide, triple port burner

1. Introduction

Increasing concerns of issues on global warning and climate change have urged stringent expectation on new energy conversion devices. In addition, effective control of flame configurations will help to improve combustion efficiency and reduce pollution emissions. For example, swirlers [1] are extensively utilized in combustion system to increase flow residence time as well as fuel-air mixing, and hence to improve flame stability. Besides, heat exchangers and flue gas recirculation mechanism [2] are generally applied in engines and furnaces to increase temperature and pressure in the flow field and to extend flammability limits. On the other hand, employing catalyst [3] to accelerate chemical reactions or imposing microwave or plasma [4] to induce active chemical radicals (H, OH) in flames are also the well-known strategies to improve combustion behavior. Nevertheless, to minimize the modification of a combustion system, an attractive alternative is to employ active fuels (such as hydrogen [5]) or to add strong oxidizer for combustion enhancement.

Hydrogen peroxide (H_2O_2) and nitrous oxide (N_2O) are often used as the oxidizer propellant for propulsion systems, because chemical dissociation reactions produce oxygen in addition to exothermic heat release. Chen et al. [6] numerically studied the effect of H_2O_2 addition on premixed methane/air flames. They found that the laminar burning velocity and adiabatic flame temperature are significantly increased due to heat release from thermal decomposition of H_2O_2. Production of radicals such as OH, H, O, and HO_2 are also enhanced. Mathieu et al. [7] found that N_2O addition to H_2/O_2 mixture decreased the ignition delay time and it was mainly due to the reaction $N_2O+M = N_2+O+M$, which provides O atoms to strengthen the reaction $O+H_2 = OH+H$. Yepes et al. [8] discovered that the laminar burning velocity increases by almost 25% with an increment of 4% oxygen in the oxidant. Ozone is known as one of the strongest oxidizers and therefore is widely used in many applications. Vu et al. [9] found that the blowoff velocity is significantly increased, and the flamability limits for both fuel-lean and fuel-rich mixtures are also extended with ozone addition. Besides, their simulation results revealed that $O_3+N_2 = O+O_2+N_2$ and $O_3+H = O_2+OH$ are the key mechanisms for the enhancement of laminar burning velocity.

Since the turbulent flames are difficult to study due to their complicated behaviors such as wrinkled shape and unsteady motion, the study of laminar simple flames may facilitate to understand the complicated turbulent combustion. According to the feeding pattern of the fuel and oxidizer, there are two types of diffusion flames: normal diffusion flame (NDF) and inverse diffusion flame (IDF), the IDF is a special flame with an inner oxidizer jet surrounded by an outer fuel jet. Shaddix et al. [10] showed that the relative positions of OH, PAH, and soot were very similar in the normal and inverse steady flames. Besides, PAH signals and soot concentrations of the IDF are somewhat smaller than those of the NDF. Liu and Smallwood [11] found that the central air jet has a significant effect on the flame structure and sooting characteristics of the flame in a three-port co-annular burner. Johnson and Sobiesiak [12] studied the hysteresis of methane inverse diffusion flame. Their numerical simultion results suggest that when the local equivalence ratio approaches to one in upstream of the flame, the partially premixed flame (PPF) propagates upstream and stabilizes as an IDF.

In order to further understand the methane/air flame with oxidizer addition which can avoid the combustion instability during operation, the strong oxidizer concept, such as employing oxy-enriched conditions and nitrous oxide (N_2O) to enhance combustion, is investigated in this study.

2. Research method

The objective of this work is to theoretically and experimentally investigate the flame behaviors of methane diffusion flames with oxy-enriched oxidizer and N_2O addition by varying the velocity ratio ($R = V_1/V_2$). Flame images and chemiluminescence techniques are used for the present study. The outer air stream velocity was maintained at 40 cm/s. The central oxygen concentration is expressed as:

$$\Omega = \left(\frac{X_{O_2}}{X_{O_2}+X_{N_2}}\right)\cdot 100\% \qquad (1)$$

The experimental apparatus is shown in Fig. 1. It consists of three concentric tubes where the oxidizer, methane, and air flow out, respectively. The flow rates of three stream were controlled using mass flow controllers (BROOKS 5850E series). To capture the flame shape, a digital camera (Nikon D80) was used. The data acquisition system and a fine 75 μm diameter R type thermocouple were used for in-flame temperature measurements. To measure the spectrum intensity from soot radiation, the emission light from the flame was guided to a spectroscope (Ocean Opitics; USB4000-UV-VIS) with an optical fiber (P100-2-UV/VIS).

The theoretical predictions of flame height and shape are based upon the triaxial burke-schumann methodology which derived from Ko et al. [13]. It is based on the fast chemistry (flame-sheet approximation), with various assumptions such as unity Lewis number, neglect of buoyancy, momentum transfer, shearing force and radiation heat transfer effects. The general solutions are obtained as follows:

$$0 = A'_{0,3} + \sum_{n=1}^{\infty} A'_{n,3}\frac{2}{\Phi_n J_0^2(\Phi_n)} J_0(\Phi_n \xi_f)\exp\left(\frac{Pe-\sqrt{Pe^2+4\Phi_n^2}}{2}\eta_f\right) \qquad (2)$$

$$A'_{0,3} = -\tilde{Y}_{3,j}\cdot\left(\frac{u_3}{u_2}\right) - c_1^2\left[\tilde{Y}_{1,j}\cdot\left(\frac{u_1}{u_2}\right)+\tilde{Y}_{2,j}\right] + c_2^2\left[\tilde{Y}_{2,j}+\tilde{Y}_{3,j}\left(\frac{u_3}{u_2}\right)\right] \qquad (3)$$

$$A'_{n,3} = c_2 J_1(c_2\Phi_n)\left[\tilde{Y}_{2,j}+\tilde{Y}_{3,j}\left(\frac{u_3}{u_2}\right)\right] - c_1 J_1(c_1\Phi_n)\left[\tilde{Y}_{1,j}\cdot\left(\frac{u_1}{u_2}\right)+\tilde{Y}_{2,j}\right] \qquad (4)$$

3. Results and Discussion

Fig. 2 depicts the theoretical predictions of the flame shape influenced by central oxidizer addition. It shows that an inner IDF and an outer NDF can be predicted by adjusting the R value. In addition, an envelope flame which the inner and outer flame stochiometric contours merge to form a single contour takes place at higher velocity ratio and oxygen concentration. Besides, Peclet number is a function of the physical properties and velocity of the stream. It is defined as:

$$Pe = \frac{\rho u_{ref} r_3}{\frac{\lambda}{C_p}} = \frac{u_{ref} r_3}{\alpha} \qquad (5)$$

Figs. 2b and 2d show that the flame shape is significantly affected by the Peclet number and stream temperature. The higher stream temperature changes the thermal diffusivity, decreases the Peclet number, and then shortens the flame height.

In the experiment, the NDF appears in very yellow-orange color for Ω = 21% as shown in Fig. 3A. By increasing the flow rate of central oxidizer, the flame appearance indicates that partial premixing reduces and ultimately eliminates soot particles in methane flames. When oxygen concentration increases to Ω = 30% and 33% (Figs. 3B and 3C), it can be seen that the blue weak curved flame front, which is a partially premixed flame, moves upstream. When the oxygen concentration increases to Ω = 35% and the velocity ratio increases to R = 6 as shown in Fig. 4, the PPF propagates upstream to ignite the IDF and the soot-free blue flame suddenly becomes a yellow-orange sooty flame again. Fig.5 shows the temperature profiles along the axial distance above the burner exit. In comparison of the flame types of R=3(PPF) and R=3(NDF&IDF), it is conjectured that the anchored IDF increases the temperatures along the flame centerline region, which greatly accelerates the pyrolysis of the fuel, leading to enhanced soot formation. If the value of R increases continuously, the open flame tip phenomenon of IDF and NDF can be observed, this is because that the fuel is consumed locally by the considerable amount of oxidizers. Furthermore, the flame shape strongly depends on the adjusting process. The extinction point of the IDF is not the same as the ignition point [12]. Fig. 6 shows the hysteresis characters of the flames for various V_2.

Fig. 7 shows the critical values of R for IDF formation under various V_2 and Ω at V_3 = 40 cm/s. It can be seen that the increase of oxygen concentration (Ω), the decrease of the R values. When N_2O is used as the oxidizer, the critical values of R for IDF formation are equivalent to the condition of Ω = 70%. Results suggest that the large heat release rate from N_2O dissociation enhances the intensity of combustion system. Fig. 8 shows the measured flame emission spectra at different flame heights when N_2O is used as the oxidizer. The measured spectra indicate that the soot intensity (from 350 to 800 nm) increases with increasing the flame height and velocity ratio. This finding suggests that N_2O addition to the flame enhances soot formation, which has been discussed in the literature [14].

4. Conclusions

In this study, the theoretical results show that the stream velocities, fuel and oxidizer concentrations and stream temperatures affect the flame structures. The experimental results reveal that the formation of the double flame structures, an inner inverse diffusion flame (IDF) and an outer normal diffusion flame (NDF), occurs only when $\Omega \geq 35\%$ and using N_2O as an oxidizer. It is conjectured that the increase of oxygen content enhances the local heat release rate to induce the partially premixed flame that propagates rapidly upstream to form the inner IDF. The increased soot formation could also be due to the changes of local velocity and temperature. Furthermore, before the formation of IDF, N_2O addition to the flame strongly favors soot formation as compared to the oxy-enriched conditions. Besides, when N_2O is used as the oxidizer, the critical values of R for IDF formation are equivalent to the condition of Ω = 70%.

5. Acknowledgement

This research was supported by the Ministry of Science and Technology of the Republic of China under the grant number MOST 103-2221-E-216 -019.

References

[1] Mattioli, R. et al., (2009). Secondary air injection in miniature liquid fuel film combustors. *Proc. Combust. Instit.* 32: 3091-3098.

[2] Majeebu, M.A. et al., (2009). Applications of porous media combustion technology – a review. *Applied Energy* 86: 1365-1375.

[3] Li, Y.H. et al., (2013). Combustion characteristics in a small-scale reactor with catalyst segmentation and cavities. *Proc. Combust. Instit.* 34: 2253-2259.

[4] Starikovskiy A. and Aleksandrov N., (2013). Plasma-assisted ignition and combustion. *Prog. Energy Combust. Sci.* 39: 61-110.

[5] Cheng, T.S. et al., (2011). An experimental and numerical study on characteristics of laminar premixed $H_2/CO/CH_4$/air flames. *International Journal of Hydrogen Energy* 36: 13207-13217.

[6] Chen, G.B. et al., (2013). Chemical effect of hydrogen peroxide addition on characteristics of methane-air combustion. *Energy* 55: 564-570.

[7] Mathieu, O. et al., (2012). Effects of N_2O addition on the ignition of H_2-O_2 mixture: Experimental and detailed kinetic modeling study. *International Journal of Hydrogen Energy* 37: 15393-15405.

[8] Yepes, H.A. and Amell, A.A. (2013). Laminar burning velocity with oxygen-enriched air of syngas produced from biomass gasification." *International Journal of Hydrogen Energy* 38: 7519-7527.

[9] Vu, T.M. et al., (2014). Stability enhancement of ozone-assisted laminar premixed Bunsen flames in nitrogen co-flow. *Combust. Flame* 161: 917-926.

[10] Shaddix, C.R. et al., (2005). Flame structure of steady and pilsed sooting inverse jet diffusion flames. *Proc. Combust. Inst.* 30: 1501-1508.

[11] Liu, F. and Smallwood, G.J., (2011). Control of the structure and sooting characteristics of a coflow laminar methane/air diffusion flame using a central air jet: An experimental and numerical study. *Proc. Combust. Instit.* 33: 1063-1070.

[12] Johnson, M.B. and Sobiesiak, A., (2011). Hysteresis of methane inverse diffusion flames with co-flowing air and combustion products. *Proc. Combust. Instit.* 33: 1079-1085.

[13] Ko, Y.C. et al., (2005). Laminar diffusion flames in a multiport burner. *Combustion Science and Technology*. 177: 1463-1484.

[14] Abian, M. et al. (2014). Impact of nitrogen oxides (NO, NO_2, N_2O) on the formation of soot. *Combust. Flame* 161: 280-287.

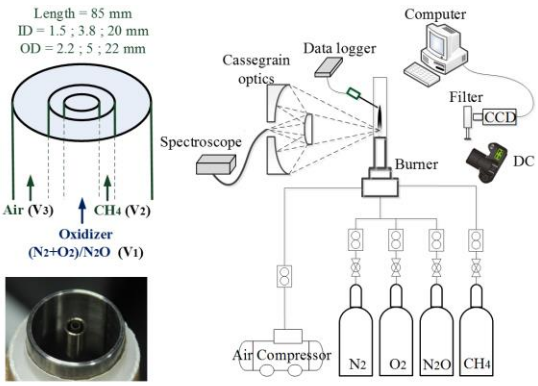

Figure 1. Experimental facility schematics.

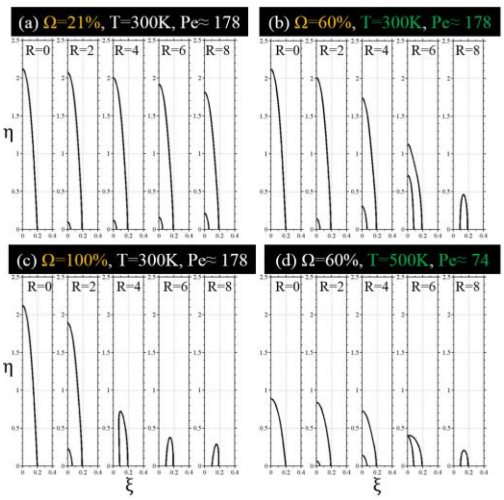

Figure 2. Predictions of flame configuration for different oxidizers, velocity ratios, and temperatures at V_2=V_3=40 cm/s.

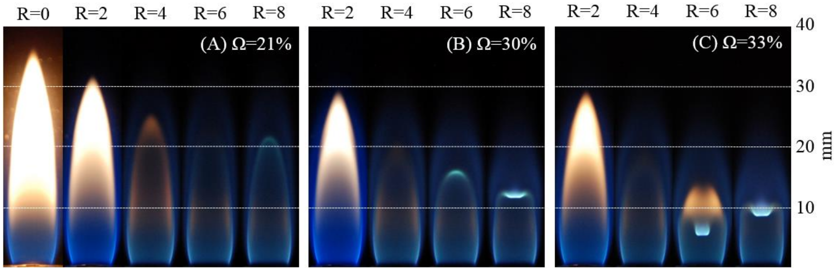

Figure 3. The visible flame appearances for V_2=V_3=40 cm/s with various R and Ω.

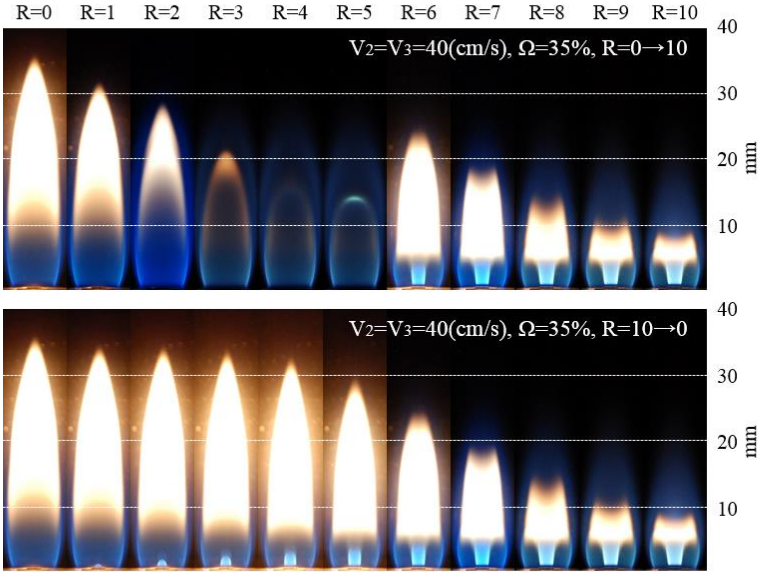

Figure 4. The visible flame appearances for V_2=V_3=40 cm/s and Ω=35% with increasing and decreasing R.

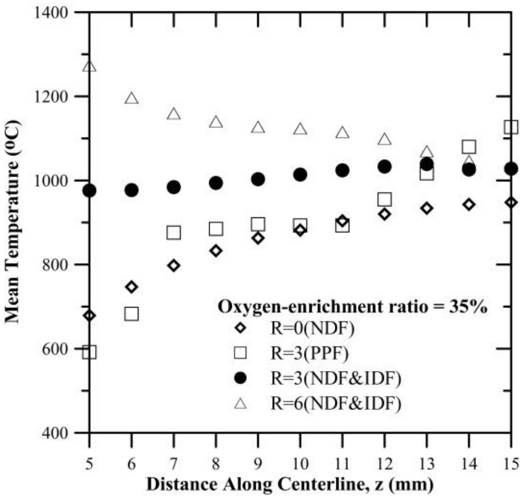

Figure 5. Mean Temperature profiles of different flame types along axial distance.

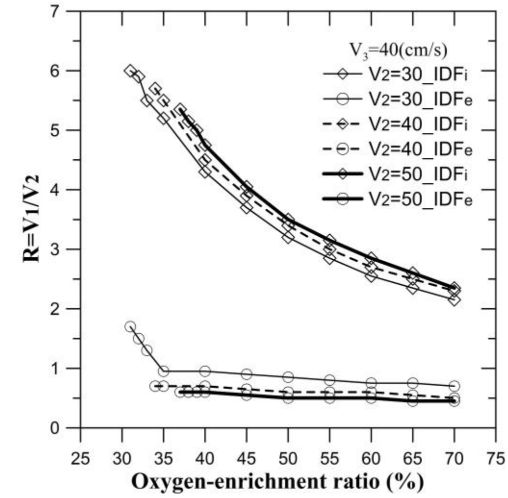

Figure 6. Velocity ratio for flame transitions from the partially premixed flame to the extinction of inverse diffusion flame with various Ω and V_2.

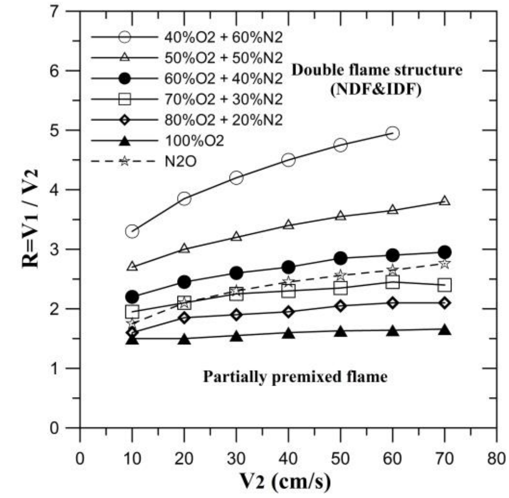

Figure 7. The critical values of R for IDF formation under various V_2 and Ω at V_3 = 40 cm/s.

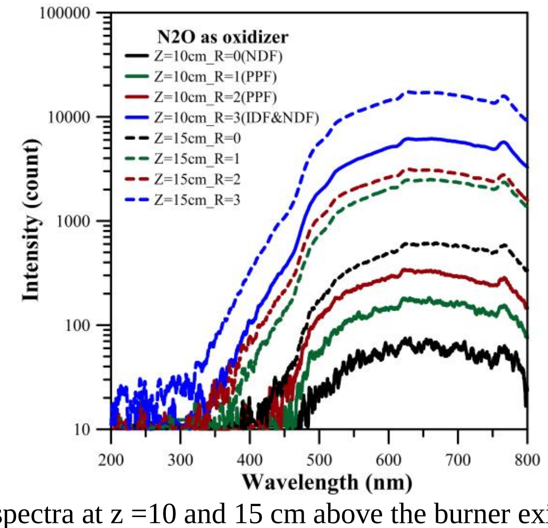

Figure 8. Flame emission spectra at z =10 and 15 cm above the burner exit with various R and N_2O as the oxidizer.